



FX Option Pricing with Stochastic-Local Volatility Model

Zili Zhu, Oscar Yu Tian, Geoffrey Lee, Xiaolin Luo, Bowie Owens and Thomas Lo

Report Number: CMIS 2013/132903

April 10, 2014

Quantitative Risk Group

Commercial In Confidence

CSIRO Mathematics, Informatics and Statistics
CSIRO Computational informatics (since Oct/2013)
Gate 5, Normanby Road, Clayton 3168, Australia
Private Bag 33, Clayton South MDC, 3169, Victoria, Australia
Telephone : +61 3 9545 8000
Fax : +61 3 9545 8080

April 10 2014: modified to reflect the change in using mixing fraction to weigh on the correlation parameter of the Heston model.

Copyright and disclaimer

© 2013 CSIRO To the extent permitted by law, all rights are reserved and no part of this publication covered by copyright may be reproduced or copied in any form or by any means except with the written permission of CSIRO.

Important disclaimer

CSIRO advises that the information contained in this publication comprises general statements based on scientific research. The reader is advised and needs to be aware that such information may be incomplete or unable to be used in any specific situation. No reliance or actions must therefore be made on that information without seeking prior expert professional, scientific and technical advice. To the extent permitted by law, CSIRO (including its employees and consultants) excludes all liability to any person for any consequences, including but not limited to all losses, damages, costs, expenses and any other compensation, arising directly or indirectly from using this publication (in part or in whole) and any information or material contained in it.

Contents

1 Introduction	1
2 Stochastic-Local Volatility Model	1
2.1 The model	1
2.2 Calibration of SLV model	2
2.2.1 Calibration of leverage function	3
2.2.2 Fokker-Planck equation	4
2.2.3 Approximation of initial condition	5
2.3 Finite difference scheme	6
2.4 Option pricing techniques	7
2.5 Complete implementation of the SLV model	8
3 Numerical Results in FX Markets	9
3.1 Implied volatility surface	9
3.2 Pricing barrier options	12
4 Summary	14

1 Introduction

The valuation of barrier options and other path-dependent options is different from that of vanilla options as the prices of these options are not dependent on the dynamics of the vanilla market quotes. The local volatility and stochastic volatility models are actually calibrated to only market vanilla options, and hence do not have the flexibility to capture the dynamics of the exotic markets.

The class of stochastic-local volatility (SLV) models in this paper is calibrated to both vanilla and exotic prices available on the market.

The SLV model we use here follows a Heston-like term-structure model. The reasons we choose a Heston-like SLV model are that: 1) a square-root process for the underlying with an mean-reverting process for the variance is widely used in the industry; 2) semi-analytic formulas (Heston [1993]) or fast pricing methods (Carr & Madan [1999] and Fang & Oosterlee [2008]) are available so that we can calibrate the stochastic parameters more efficiently.

2 Stochastic-Local Volatility Model

2.1 The model

The stochastic-local volatility (SLV) model is assumed to follow Heston-like dynamics for the spot price S_t and for the stochastic variance V_t as

$$\begin{aligned}dS_t &= [r_d(t) - r_f(t)]S_t dt + L(S_t, t)\sqrt{V_t}S_t dW_t^1, S_0 = s, \\dV_t &= \kappa(\theta - V_t)dt + \lambda\sqrt{V_t}dW_t^2, V_0 = v, \\dW_t^1 \cdot dW_t^2 &= \rho dt.\end{aligned}\tag{2.1}$$

where $r_d(t)$ is domestic interest rate and $r_f(t)$ is foreign interest rate in the context of FX markets, both of which are assumed to be of term structure. We will denote $r(t) = r_d(t) - r_f(t)$ in the rest of the paper. We also assume that the stochastic parameters (κ, θ, λ and ρ) in the SLV model have term structures.

Here $L(S_t, t)$ is called leverage function, which is numerically calibrated to the market data. $L(S_t, t)$ represents the weight of local volatility.

Now we focus on the construction of the leverage function starting from the computation of the local volatility. Suppose we have a local volatility model

$$dS_t = r(t)S_t dt + \sigma_{LV}(S_t, t)S_t dW_t.\tag{2.2}$$

Given market prices of the call options $C(K, T|S_0)$, we can derive the local volatility $\sigma_{LV}(S, t)$ at the maturity T from Dupire's equation (see Dupire [1994])

$$\sigma_{LV}(S, t) = \sqrt{\frac{\frac{\partial C}{\partial T} + rK \frac{\partial C}{\partial K} + r_f C}{\frac{K^2}{2} \frac{\partial^2 C}{\partial K^2}}} \Bigg|_{K=S, T=t}.\tag{2.3}$$

Alternatively, given the implied volatility $\sigma_{IV}(K, T|S_0)$ in the Black-Scholes formula, we can derive the local volatility $\sigma_{LV}(S, t)$ from the implied volatility as (see, e.g., Wilmott [2006]) and

Gatheral [2006])

$$\sigma_{LV}(S, t) = \sqrt{\frac{\sigma_{IV}^2 + 2\sigma_{IV}T\frac{\partial\sigma_{IV}}{\partial T} + 2r\sigma_{IV}TK\frac{\partial\sigma_{IV}}{\partial K}}{(1 + d_1K\sqrt{T}\frac{\partial\sigma_{IV}}{\partial K})^2 + \sigma_{IV}K^2T[\frac{\partial^2\sigma_{IV}}{\partial K^2} - d_1(S_0, K)\sqrt{T}(\frac{\partial\sigma_{IV}}{\partial K})^2]}} \Big|_{K=S, T=t}, \quad (2.4)$$

where

$$d_1(S_0, K) = \frac{\log(S_0/K) + [r + \sigma_{IV}^2/2]T}{\sigma_{IV}\sqrt{T}}. \quad (2.5)$$

If we want the price process of the new SLV model to mimic that of the local volatility model and hence they generate the same pricing results for European options, i.e., the so-called market prices, we should match the diffusion terms of the two models.

Given the transition probability of the SLV model $p(S_t, V_t, t)$ and the transition probability of the LV model $p_{LV}(S_t, t)$, we can connect the local volatility with the the volatility part in model (2.1) by the following mimicking theorem:

To mimic the LV model (2.2), the diffusion term in the SLV model (2.1) follows

$$\sigma_{LV}(x, t)^2 = \mathbb{E}[L(S_t, t)^2 V_t | S_t = x] = L(x, t)^2 \mathbb{E}[V_t | S_t = x], \quad (2.6)$$

Furthermore, the probability distribution of the LV model (2.2) is the same as the marginal probability distribution of the SLV model (2.1) and we have the relation between the transition probability densities

$$p_{LV}(S, t) = \int_0^{+\infty} p(S, V, t) dV. \quad (2.7)$$

We refer to Gyöngy [1986] and Tachet [2011] for a detailed proof.

Since the price of vanilla options only depends on the final state of the spot price and the market prices for vanilla options (or market implied volatilities) yield the local volatility, therefore the pricing results for vanilla options from the new SLV model with the above properties should match the market prices for vanilla options.

For now, we have the leverage function

$$L(x, t) = \frac{\sigma_{LV}(x, t)}{\sqrt{\mathbb{E}[V_t | S_t = x]}}, \quad (2.8)$$

which can be roughly seen as a ratio between local volatility and the conditional expectation of stochastic volatility.

From the above relation (2.8), we infer that when $L(S_t, t) \equiv 1$ the SLV model (2.1) becomes the pure Heston stochastic volatility model; and when the vol of vol $\lambda \equiv 0$ the process for V_t becomes deterministic with $L = \frac{\sigma_{LV}}{\sqrt{V_t}}$, the SLV model degenerates to the pure local volatility model.

After calibration of the stochastic parameters and the leverage function, the SLV model can be used to reproduce the implied volatility surface and price exotic options.

2.2 Calibration of SLV model

We now present our implementation of calibrating the SLV model. There are two sets of parameters to be calibrated, the Heston stochastic parameters (κ, θ, λ and ρ) and the leverage function L .

If we calibrate the Heston stochastic parameters to the market implied volatility data for around ATM strikes, then the pure stochastic volatility model could explain the given market implied volatility data. However, we should note that the pure stochastic volatility model cannot explain the whole market implied volatility surface, especially for far-end strikes.

When the leverage function is introduced to consider the effect of the local volatility component, it could correct the far-end implied volatilities from the stochastic volatility model in the right direction towards the market implied volatilities. We should also note that the vol of vol λ mainly determines the impact of stochastic volatility: when the vol of vol λ stays at a high level, the impact of the local volatility disappears; when $\lambda = 0$, the local volatility dominates.

To control the impact of stochastic volatility and local volatility, a so-called mixing fraction weight $\eta \in [0, 1]$ is introduced (see, e.g., Tataru & Fisher [2010] and Clark [2011]) to multiply the vol of vol λ . For calibrated stochastic parameters, when $\eta = 1$, the stochastic volatility component dominates and the local volatility implied by the leverage function has little effect; when $\eta = 0$, the local volatility component dominates; when $0 < \eta < 1$, both work together.

For the mixing fraction weight, different researchers have very different opinions. Tataru & Fisher [2010] propose to use the normalized risk reversal moves to infer the term structure of η . Clark [2011] suggest that it is typically set to be around 0.60 or 0.65.

In our implementation, we suggest to give an interval of η that could calibrate the leverage function to the market implied volatilities within a satisfactory tolerance level and then find the optimal by matching market prices of some exotic options.

So now the calibration procedure of the SLV model consists of two main steps: 1) find the stochastic parameters of the pure Heston model to match given market implied volatility data; 2) then calibrate leverage function L with a proper mixing fraction ratio η .

For the first stage, the Heston semi-analytic pricing formula (see, e.g., Heston [1993] and Mikhailov & Nögel [2003]), Fourier transform method (see Carr & Madan [1999]) and the COS method proposed by Fang & Oosterlee [2008] can be used to achieve fast and accurate calibration for the term-structure Heston model as long as the characteristic function of the model is available, see Elices [2009]. A nonlinear least squares optimization (e.g., Levenberg-Marquardt algorithm) is performed to find the optimal parameters.

2.2.1 Calibration of leverage function

The idea of calibrating the leverage function is as follows. When looking into formula (2.8) for the leverage function, we can actually express the conditional expectation in the formula as integrals involving transition probability densities of the SLV model. We also know that the Fokker-Planck equation describes the evolution of this transition probability density. So if we can solve the Fokker-Planck equation, we can evaluate the leverage function via integrals of the probability densities.

For the second stage, once the Heston model parameters are determined by its calibration, the mixing fraction is applied to both the vol of vol and also to the correlation ρ for each maturity tenor (for which vanilla and possible exotic options are the market data input during calibration). The local volatility surface value and the Fokker-Planck equation are computed and used to generate the probability density function and leverage function, and then the leverage function can be used to price the input known market vanillas and exotics, the mixing fraction that gives the smallest overall errors is chosen. The same procedure is repeated for the next maturity until all

maturity tenors are calibrated. In this stage, a one-dimensional nonlinear optimizer, e.g., golden section search, can be used to optimize the mixing fraction, and the leverage function is thus determined.

The reason for adding exotic prices to the calibration process is to match the dynamics of the volatility surface as underlying spot moves. In the equities market, SLV models are primarily used to completely match the observed implied volatility smiles, whereas in FX markets, SLV models are used to represent the dynamics of volatility.

Here exotic prices are treated just like the vanilla prices: i.e. errors for exotic prices and vanillas are minimized to find the mixing fraction by an optimizer. There is a choice for using different weights on exotic prices to vanilla prices, for example, we can regard one exotic price is worth three times the weight for a vanilla.

It should be noted that, as the process for V_t is a square-root process, the Feller condition $2\kappa\theta > \lambda^2$ is required to preserve the positivity of the variance process. However, the Feller condition is often violated in the real market (see Clark [2011] and Janek, Kluge, Weron & Wystup [2011] for some examples in the FX markets) and this can cause wrong calculations of the probability distribution. For example, Fang & Oosterlee [2011] have shown that when the Feller condition is violated, the decay rate of the variance density will increase dramatically when V_t approaches zero, and hence, they propose to use the log-variance domain instead.

To maintain the positivity of the variance process, we transform the original SLV model of (S_t, V_t) into a model of log-spot and log-variance as $(X_t = \log(S_t/S_0), Z_t = \log(V_t/V_0))$ in the log-domain, which is also scaled by the initial point (S_0, V_0) .

From Ito's lemma, we then have the SLV model for the log-spot X_t and the log-variance Z_t as

$$\begin{aligned} dX_t &= [r_d(t) - r_f(t) - \frac{1}{2}L(X_t, t)^2V_t]dt + L(X_t, t)\sqrt{V_t}dW_t^1, \quad X_0 = 0, \\ dZ_t &= [(\kappa\theta - \frac{1}{2}\lambda^2)\frac{1}{V_t} - \kappa]dt + \lambda\frac{1}{\sqrt{V_t}}dW_t^2, \quad Z_0 = 0, \\ dW_t^1 \cdot dW_t^2 &= \rho dt. \end{aligned} \quad (2.9)$$

Here $L(X_t, t) := L(S_0 \cdot e^{X_t}, t) = L(S_t, t)$, $S_t = S_0 \cdot e^{X_t}$ and $V_t = V_0 \cdot e^{Z_t}$.

2.2.2 Fokker-Planck equation

From the Fokker-Planck equation (or the Kolmogorov forward PDE) for the transition probability density $p(X_t, Z_t, t)$ in the SLV model (2.9), we have

$$\begin{aligned} \frac{\partial p}{\partial t} &= -\frac{\partial}{\partial X}[(r(t) - \frac{1}{2}L^2V)p] - \frac{\partial}{\partial Z}[(\kappa\theta - \frac{1}{2}\lambda^2)\frac{1}{V} - \kappa]p + \\ &+ \frac{1}{2}\frac{\partial^2}{\partial X^2}[L^2Vp] + \frac{\partial^2}{\partial X\partial Z}[\lambda\rho Lp] + \frac{1}{2}\frac{\partial^2}{\partial Z^2}[\lambda^2\frac{1}{V}p], \end{aligned} \quad (2.10)$$

with the initial condition (we now have $X_0 = 0, V_0 = 0$)

$$p(X, Z, 0) = \delta(X) \cdot \delta(Z), \quad (2.11)$$

where $\delta(\cdot)$ is the Dirac delta function. This is an initial value problem with free boundary condition.

We also know that from equation (2.8)

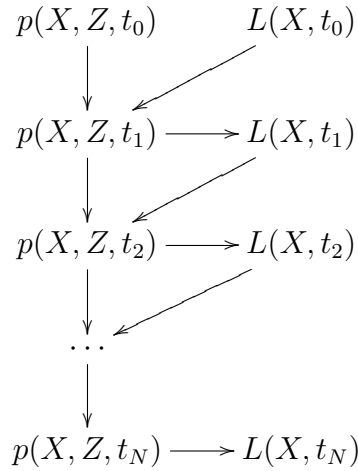
$$L(X, t) = \frac{\sigma_{LV}(X, t)}{\sqrt{\mathbb{E}[V|X]}} = \sigma_{LV}(X, t) \sqrt{\frac{\int_{-\infty}^{+\infty} p(X, Z, t) dZ}{\int_{-\infty}^{+\infty} V p(X, Z, t) dZ}}. \quad (2.12)$$

In particular, at time 0, we have

$$L(X, 0) = \frac{\sigma_{LV}(X, 0)}{\sqrt{V_0}}. \quad (2.13)$$

Note that only the initial values of p and L are known from (2.11) and (2.13) at this stage, whereas they are unknown for any future times. However, at a future time t , given $p(X, Z, 0)$ and $L(X, 0)$, we can solve (2.10) for $p(X, Z, t)$ and then find $L(X, t)$ by evaluating (2.12) afterwards. Hence, given a series of time points $t_0 (= 0), t_1, \dots, t_N (= T)$, we can start from $p(X, Z, t_0)$ and $L(X, t_0)$ to calculate $p(X, Z, t_1)$ by solving PDE (2.10) one step forward in time and to evaluate $L(X, t_1)$ via equation (2.12). In this alternate procedure, we can obtain $L(X, t_n)$ as well as $p(X, Z, t_n)$ till maturity, $n = 0, 1, \dots, N$. The procedure is illustrated in Figure 2.1.

Figure 2.1: Calibration procedure for leverage function



2.2.3 Approximation of initial condition

To solve PDE (2.10) in a finite difference framework, we discretise the transition probability $p(X, Z, t)$ in the X - and Z -directions as $p_{i,j}^n = p(X_i, Z_j, t_n)$.

We assume that the transition probability $p(X_i, Z_j, 0)$ at the initial time can be approximated by that of a bivariate normal distribution at a small forward time Δt as

$$p_{i,j}^0 = p(X_i, Z_j, 0) \approx \frac{1}{2\pi\sigma_X\sigma_Z\sqrt{1-\rho^2}} \cdot \exp\left(-\frac{\frac{(X_i-\mu_X)^2}{\sigma_X^2} + \frac{(Z_j-\mu_Z)^2}{\sigma_Z^2} - \frac{2\rho(X_i-\mu_X)(Z_j-\mu_Z)}{\sigma_X\sigma_Z}}{2(1-\rho^2)}\right), \quad (2.14)$$

with

$$\begin{aligned} \mu_X &= [r(0) - \frac{1}{2}L(0,0)^2v]\Delta t, \quad \sigma_X = L(0,0)\sqrt{v\Delta t}, \\ \mu_Z &= [(\kappa\theta - \frac{1}{2}\lambda^2)\frac{1}{v} - \kappa]\Delta t, \quad \sigma_V = \lambda\sqrt{\frac{\Delta t}{v}}. \end{aligned} \quad (2.15)$$

As $\Delta t \rightarrow 0$, the above probability density converges to Dirac delta function in the initial condition (2.11).

Hence, the leverage function (2.12) can be approximated by using the trapezoidal rule as

$$L(X_i, t_n) \approx \sigma_{LV}(X_i, t_n) \sqrt{\frac{\frac{1}{2} \sum_{j=1}^{N_Z} (p_{i,j}^n + p_{i,j+1}^n) \Delta Z}{\frac{1}{2} \sum_{j=1}^{N_Z} (V_j p_{i,j}^n + V_{j+1} p_{i,j+1}^n) \Delta Z}} \quad (2.16)$$

Given a uniformly spaced mesh, we can further simplify it as

$$L(X_i, t_n) \approx \sigma_{LV}(X_i, t_n) \sqrt{\frac{\sum_{j=1}^{N_Z} (p_{i,j}^n + p_{i,j+1}^n)}{\sum_{j=1}^{N_Z} (V_j p_{i,j}^n + V_{j+1} p_{i,j+1}^n)}}. \quad (2.17)$$

Since we have that $\int_{-\infty}^{+\infty} \int_{-\infty}^{+\infty} p(X, Z, 0) dZ dX = 1$ at the initial time, we choose a small Δt such that

$$\sum_{i=1}^{N_X} \sum_{j=1}^{N_Z} \frac{1}{4} (p_{i,j}^0 + p_{i+1,j}^0 + p_{i,j+1}^0 + p_{i+1,j+1}^0) \Delta X \Delta Z \approx 1, \quad (2.18)$$

by using the trapezoidal rule in two dimensions. At each time step, we should have similar results.

The advantages of this approach are that: firstly, we have a number of nodes around the initial point $(0, 0)$ in the log-domain with non-zero probability densities by using a normal approximation, which will increase the stability in solving PDE (2.10); and secondly, this approach also works with a non-uniform mesh.

2.3 Finite difference scheme

In this section, we discuss the finite difference method used to solve Fokker-Planck equation for the SLV model. We refer to Tavella & Randall [2000] and in't Hout & Foulson [2010] for more details on this topic.

To solve the initial value problem (2.10), the alternating-direction-implicit (ADI) method can be used. Tataru & Fisher [2010] suggest to use a modified Douglas scheme from in't Hout & Foulson [2010] to solve the initial value problem (2.10) as:

$$\begin{aligned} A &= p^{n-1} + \Delta t_n [F_0(p^{n-1}, t_{n-1}) + F_1(p^{n-1}, t_{n-1}) + F_2(p^{n-1}, t_{n-1})], \\ B - \alpha \Delta t_n F_1(B, t_n) &= A - \alpha \Delta t_n F_1(p^{n-1}, t_{n-1}), \\ C - \alpha \Delta t_n F_2(C, t_n) &= B - \alpha \Delta t_n F_2(p^{n-1}, t_{n-1}), \\ p^n &= C, \quad n = 1, \dots, N, \end{aligned} \quad (2.19)$$

with F_0 , F_1 and F_2 representing the derivative terms in the mixed derivative, Z - and X -directions, respectively (see expression (2.20)). The parameter α affects the stability and accuracy of the ADI method, which lies in the range $[0, 1]$. When $\alpha = 0$, the scheme becomes fully explicit; and

when $\alpha = 1$, it is fully implicit.

$$\begin{aligned}
F_0(p, t) &= \frac{\partial^2}{\partial X \partial Z} [\lambda \rho L p], \\
F_1(p, t) &= -\frac{\partial}{\partial Z} \left[(\kappa \theta - \frac{1}{2} \lambda^2) \frac{1}{V} - \kappa \right] p + \frac{1}{2} \frac{\partial^2}{\partial Z^2} \left[\lambda^2 \frac{1}{V} p \right], \\
F_2(p, t) &= -\frac{\partial}{\partial X} \left[(r(t) - \frac{1}{2} L^2 V) p \right] + \frac{1}{2} \frac{\partial^2}{\partial X^2} [L^2 V p].
\end{aligned} \tag{2.20}$$

Here we define $\Delta t_n = t_n - t_{n-1}$, $n = 1, \dots, N$ as a variable step size. The reason to use a variable time step size is that: we usually have dense market data for short maturity time less than 1 year in the real market and sparse data for long maturity time, and the first few time steps determines the general shape of the transition probability, hence we can use small time steps for short maturities and large steps for long maturities so that we could obtain a good resolution of the probability density distribution and achieve a robust calibration of the leverage function.

One must be aware however, that in the above ADI method, we will use the discrete version of the leverage function L^n at a future time t_n , which is however unknown, to calculate p^n . There are several ways to approximate it. The first approach is to use the previous discrete version L^{n-1} to replace L^n . The second approach is to use the previous version of the transition probability p^{n-1} to calculate L^n by equation (2.16). Moreover, it is noted that A , B and C are all approximates of p^n , we can use the latest approximate to replace p^n involved in the calculation of L^n . Clark [2011] suggests to use the leverage function with the same moneyness from the previous time step to approximate L^n .

The transition probability density in the local volatility model should satisfy the relation $p_{LV}(X, t) = \int_{-\infty}^{\infty} p(X, Z, t) dZ$ for log-spot X , which implies that alternatively we can solve the Fokker-Planck equation for p_{LV} to replace the integral $\int_{-\infty}^{\infty} p(X, Z, t) dZ$ involved in (2.12).

Furthermore, since we do not impose boundary conditions to the initial value problem (2.10), we will use one-sided first order derivatives and zero second derivatives for boundary points in X - and Z -directions.

2.4 Option pricing techniques

Let $\tau = T - t$, then the backward option pricing PDE for a payoff function u under the SLV model (2.9) becomes:

$$\begin{aligned}
\frac{\partial u}{\partial \tau} &= [r(\tau) - \frac{1}{2} L^2 V] \frac{\partial u}{\partial X} + \frac{1}{2} L^2 V \frac{\partial^2 u}{\partial X^2} + \lambda \rho L \frac{\partial^2 u}{\partial X \partial Z} + \\
&+ [(\kappa \theta - \frac{1}{2} \lambda^2) \frac{1}{V} - \kappa] \frac{\partial u}{\partial Z} + \frac{1}{2} \lambda^2 \frac{1}{V} \frac{\partial^2 u}{\partial Z^2} - r_d(\tau) u.
\end{aligned} \tag{2.21}$$

For the above PDE (2.21), we use an ADI scheme similar to (2.19) as

$$\begin{aligned}
A &= u^{n-1} + \Delta \tau_n [G_0(u^{n-1}, \tau_{n-1}) + G_1(u^{n-1}, \tau_{n-1}) + G_2(u^{n-1}, \tau_{n-1})], \\
B - \alpha \Delta \tau_n G_1(B, \tau_n) &= A - \alpha \Delta \tau_n G_1(u^{n-1}, \tau_{n-1}), \\
C - \alpha \Delta \tau_n G_2(C, \tau_n) &= B - \alpha \Delta \tau_n G_2(u^{n-1}, \tau_{n-1}), \\
u^n &= C, \quad n = 1, \dots, N,
\end{aligned} \tag{2.22}$$

with

$$\begin{aligned}
 G_0(u, \tau) &= \lambda \rho L \frac{\partial^2 u}{\partial X \partial Z} + b_0(\tau), \\
 G_1(u, \tau) &= [(\kappa \theta - \frac{1}{2} \lambda^2) \frac{1}{V} - \kappa] \frac{\partial u}{\partial Z} + \frac{1}{2} \lambda^2 \frac{1}{V} \frac{\partial^2 u}{\partial Z^2} - \frac{1}{2} r_d(\tau) u + b_1(\tau), \\
 G_2(u, \tau) &= [r(\tau) - \frac{1}{2} L^2 V] \frac{\partial u}{\partial X} + \frac{1}{2} L^2 V \frac{\partial^2 u}{\partial X^2} - \frac{1}{2} r_d(\tau) u + b_2(\tau).
 \end{aligned} \tag{2.23}$$

where $b_i(\tau)$ are boundary conditions imposed on the mixed derivative, Z - and X -directions. Given proper initial conditions and boundary conditions, we can solve the above PDE to obtain option prices.

Generally, we impose zero second derivative condition and one-sided finite difference for first derivative. When there is a boundary condition for different option types, we normally use central finite difference; or one-sided difference accordingly (e.g., barrier options).

For European options with strike K , we have the initial condition for the payoff as

$$u(X_i, Z_j, 0) = \begin{cases} \max(S_0 \cdot \exp(X_i) - K, 0), & \text{for call;} \\ \max(K - S_0 \cdot \exp(X_i), 0), & \text{for put.} \end{cases} \tag{2.24}$$

For knock-in type barrier options, we have initial condition

$$u(X_i, Z_j, 0) = 0. \tag{2.25}$$

The boundary condition for a cash one-touch option with barrier B reads

$$b(\log(B), Z_j, \tau) = \exp\left(-\int_0^\tau r_d(t) dt\right). \tag{2.26}$$

For knock-in call or put options with barrier B and strike K , we have boundary condition

$$b(\log(B), Z_j, \tau) = \begin{cases} V_{call}(B, K, \tau), & \text{for call;} \\ V_{put}(B, K, \tau), & \text{for put.} \end{cases} \tag{2.27}$$

Here $V(B, K, \tau)$ represents the price of the European option with spot B , strike K and maturity τ .

Note that given the calibrated leverage function in terms of a mesh used in the calibration phase, we need to interpolate the leverage function to accommodate a new spot mesh or a new time mesh for pricing options. We suggest to use cubic spline interpolation in spot direction and linear interpolation in time direction.

2.5 Complete implementation of the SLV model

To summarize, we have the following implementation of the SLV model:

1. Calibration:

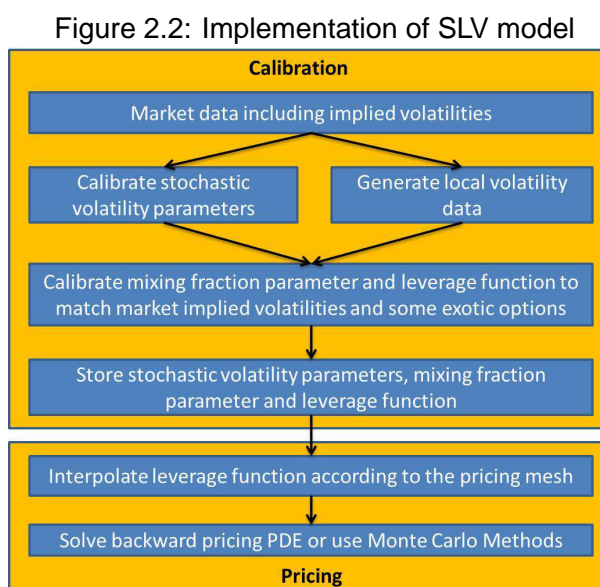
- (1) For given market data including strikes and implied volatilities, calibrate the parameters (and the initial variance) in term-structure forms for Heston stochastic volatility model.
- (2) For the same market data, generate local volatility data.

- (3) With the calibrated stochastic volatility parameters and generated local volatility, calibrate term-structure mixing fraction parameters and leverage function by solving the Fokker-Planck equation to match market implied volatilities as well as traded prices of available market exotic options.

2. Pricing:

- (1) Interpolate leverage function data along spot direction (cubic spline interpolation) or time direction (linear interpolation).
- (2) Solve backward option pricing PDE or use Monte Carlo simulation with stochastic volatility parameters, mixing fraction parameter and interpolated leverage function.

Note that the first two steps in the calibration are independent and both steps feed the third calibration step, see Figure 2.2.



3 Numerical Results in FX Markets

In this section, we will evaluate the pricing performance of the stochastic-local volatility model. Here we give an example of the EUR/USD exchange rate.

3.1 Implied volatility surface

First, we calibrate the parameters of the SLV model to market data on EUR/USD. Details of traded market prices are listed in Tables 3.1 and 3.2. We will set $\alpha = 0.5$ in the ADI method to achieve a reasonable stability.

Note that since the yields are quoted annually, we need to convert them to local forward rate, which is a function of time so that we can use the local forward rate in the finite difference method.

The market implied volatility surface are presented in terms of strikes and maturities for 5 strikes and 10 maturities in Figure 3.1. From Figure 3.1, we can see that EUR/USD data is left-skewed with higher volatilities for ITM strikes than OTM strikes. In order to represent the left-skewness of the EUR/USD data, a negative ρ should be used in the SLV model.

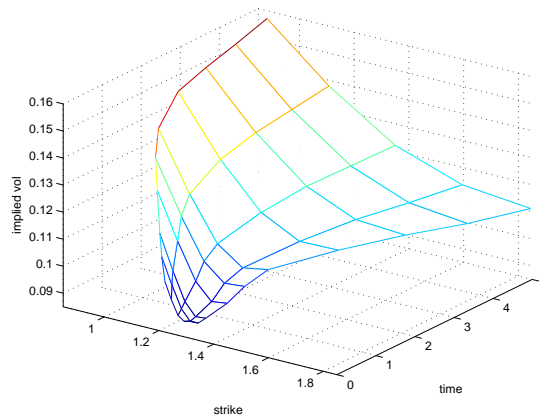
Table 3.1: EUR/USD parameter settings

Domestic currency	USD
Foreign currency	EUR
Date	23 August, 2012
Spot	1.257 USD per EUR
Delta type	Spot delta for up to 1y, driftless delta for more than 1y
ATM volatility	0-delta straddle

Table 3.2: EUR/USD market data (in %)

Maturity	Domestic yield	Foreign yield	10- Δ BF	25- Δ BF	σ_{ATM}	25- Δ RR	10- Δ RR
1m	0.4074	0.0424	0.5125	0.1713	9.1500	-0.6825	-1.2175
2m	0.5148	0.1061	0.6955	0.2175	9.3250	-1.1825	-2.1150
3m	0.6619	0.2344	0.9375	0.2813	9.5500	-1.5025	-2.7300
6m	0.9526	0.4683	1.2500	0.3600	10.1250	-1.9200	-3.5525
9m	1.1923	1.6160	1.4168	0.4200	10.6750	-2.0975	-3.9350
1y	1.1607	0.6352	1.6235	0.4675	11.1750	-2.2500	-4.2150
2y	0.5982	0.0291	1.5188	0.4425	11.6750	-2.3150	-4.3975
3y	0.7174	0.0291	1.2815	0.3688	12.0000	-2.3000	-4.3650
4y	0.7174	0.0291	1.1900	0.3565	12.1000	-2.3750	-4.5000
5y	0.7174	0.0291	1.2125	0.3750	12.2000	-2.4250	-4.6000

Figure 3.1: EUR/USD market implied volatility surface



We will compute the local volatility data, derived via Dupire's formula from the supplied market implied volatility data, see Figure 3.2, and we use the local volatility data as an input for calibrating the leverage function.

For the calibration of the SLV model, we use the scaled log-spot $X = \log(S/S_0)$ as log-moneyness and scaled log-variance $Z = \log(V/V_0)$. Here we have $S_0 = 1.257$ and $V_0 = 0.008$. We calibrate the term-structure Heston model to the market implied volatility data to get the piecewise constant stochastic parameters from the Heston model.

For the second phase, the mixing fraction weight η and the leverage function L are calibrated to the market implied volatility surface. We use the ADI method to solve the Fokker-Planck equation (2.10) numerically with the initial condition approximated by a bivariate normal distribution. The transition probability at the initial time and at a future time are shown in Figure 3.3. We can see that the fat tail in the probability distribution is noticeable in the log-domain.

The term-structure parameters of the SLV model are calibrated to the market implied volatility surface, and are listed in Table 3.3.

Although the Heston model can reproduce the implied volatilities around ATM region, it cannot

Figure 3.2: EUR/USD local volatility

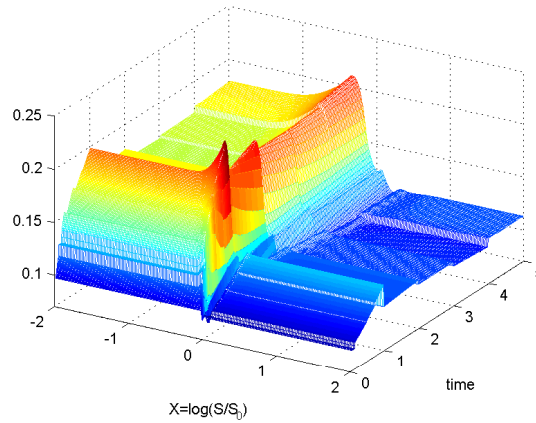


Figure 3.3: Transition probability

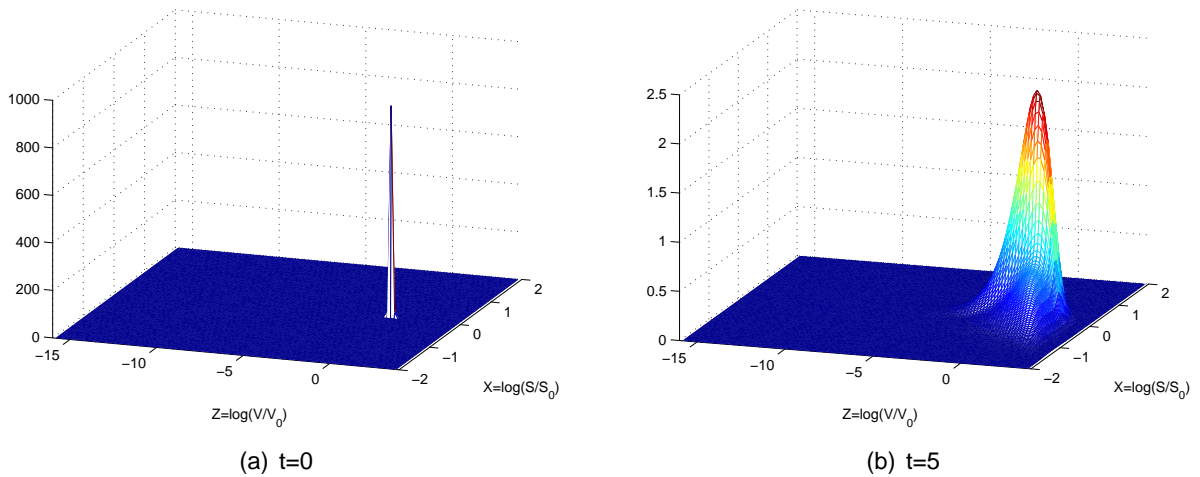


Table 3.3: Term-structure parameters in the SLV model for EUR/USD

Period	κ	θ	λ	ρ	η
0-1m	0.885	0.031	0.342	-0.288	0.796
1m-2m	0.881	0.030	0.471	-0.534	0.202
2m-3m	0.851	0.034	0.450	-0.490	0.796
3m-6m	0.816	0.039	0.430	-0.474	0.502
6m-9m	0.842	0.035	0.445	-0.489	0.611
9m-1y	1.204	0.020	0.418	-0.532	0.344
1y-2y	1.268	0.022	0.396	-0.576	0.608
2y-3y	1.166	0.022	0.439	-0.610	0.521
3y-4y	0.989	0.025	0.477	-0.582	0.448
4y-5y	0.978	0.022	0.499	-0.516	0.419

adequately match the implied volatilities at ITM or OTM regions, while the local volatility component introduced into the stochastic volatility model can correct the reproduced implied volatilities at ITM and OTM regions so as to match the whole implied volatility surface.

In Table 3.4, we present the calibrated implied volatilities in terms of 5 different deltas and 10 maturities with corresponding absolute errors in square brackets. The root mean square error (RMSE) is around 7 basis points (bps), with the mean absolute error 4 bps and maximum ab-

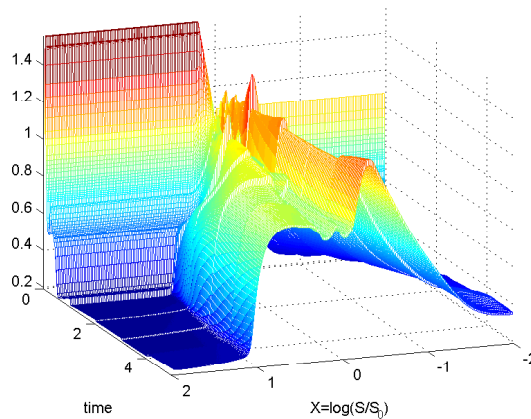
Table 3.4: Calibrated implied volatility surface from SLV for EUR/USD (in %)

Tenor	10- Δ put	25- Δ put	ATM	25- Δ call	10- Δ call
1m	10.53[-0.26]	9.88[0.22]	9.34[-0.19]	9.11[-0.13]	9.16[-0.11]
2m	11.04[0.04]	10.12[0.02]	9.41[-0.08]	8.94[0.01]	8.98[-0.01]
3m	11.89[-0.03]	10.65[-0.07]	9.64[-0.09]	9.10[-0.02]	9.15[-0.03]
6m	13.21[-0.05]	11.49[-0.04]	10.12[0.01]	9.51[0.02]	9.61[-0.01]
9m	14.08[-0.02]	12.15[-0.01]	10.73[-0.05]	10.04[0.01]	10.12[0.00]
1y	14.91[-0.01]	12.78[-0.01]	11.20[-0.02]	10.51[0.01]	10.69[0.01]
2y	15.41[-0.02]	13.31[-0.04]	11.71[-0.04]	10.97[-0.01]	10.99[0.01]
3y	15.49[-0.03]	13.55[-0.03]	12.03[-0.03]	11.23[-0.01]	11.09[0.01]
4y	15.55[-0.01]	13.65[-0.01]	12.11[-0.01]	11.27[0.00]	11.04[0.00]
5y	15.72[-0.01]	13.80[-0.02]	12.21[-0.01]	11.37[0.00]	11.11[0.00]

solute error 26 bps. The numerical results show that the SLV model could capture the whole surface well.

Figure 3.4 shows the leverage function for EUR/USD, which implied the changes of the ratio between local volatility and conditional expectation of stochastic volatility.

Figure 3.4: EUR/USD leverage function



3.2 Pricing barrier options

After calibration, we will use the SLV model to price exotic barrier options. First we compare the pricing results from the SLV model with the local volatility model for some single-barrier cash one-touch options. The details of the one-touch options are listed in Table 3.5.

Table 3.5: Parameter settings for EUR/USD single-barrier domestic one-touch options

Maturity	1m, 3m, 6m and 1y
Spot	1.257 USD per EUR
Payout	in USD
Lower trigger	$L = 1, 1.05, 1.1, 1.15$ and 1.2
Upper trigger	$U = 1.275, 1.3, 1.35$ and 1.4

In Table 3.6, we present pricing results of the one-touch options from the SLV model, the pure LV model and the pure Heston SV model. We also provide theoretical value (TV) using Black-Scholes model with constant ATM volatility (see Hakala & Wystup [2007]) for comparison. The reference prices are obtained from FENICS, which can be seen as the benchmark prices for these one-touch options. The one-touch options with barriers $L = 1.2$ and $U = 1.3$ are actually also used in the calibration phase for computing the mixing fraction and the leverage function.

We can see that if we use only constant ATM volatility, we will misprice one-touch options, especially those with barrier far away from the spot. The pricing results of the SLV model are closer to the reference prices and outperforms the pure LV and SV models in most cases.

Table 3.6: Pricing results of EUR/USD single-barrier domestic one-touch options

Maturity	Trigger	Reference	LV	SLV	SV	TV
1m	$L = 1$	0.0000	0.0000	0.0000	0.0000	0.0000
	$L = 1.05$	0.0000	0.0000	0.0000	0.0000	0.0000
	$L = 1.1$	0.0002	0.0000	0.0001	0.0006	0.0000
	$L = 1.15$	0.0076	0.0046	0.0050	0.0102	0.0007
	$L = 1.2$	0.1137	0.1200	0.1150	0.1164	0.0788
	$U = 1.275$	0.5718	0.5901	0.5706	0.5564	0.5809
	$U = 1.3$	0.1859	0.1943	0.1808	0.1725	0.1977
	$U = 1.35$	0.0096	0.0071	0.0080	0.0090	0.0065
3m	$L = 1$	0.0011	0.0004	0.0004	0.0032	0.0000
	$L = 1.05$	0.0070	0.0050	0.0049	0.0111	0.0001
	$L = 1.1$	0.0319	0.0336	0.0328	0.0363	0.0032
	$L = 1.15$	0.1096	0.1262	0.1242	0.1104	0.0489
	$L = 1.2$	0.3274	0.3515	0.3456	0.3191	0.3043
	$U = 1.275$	0.7578	0.7815	0.7560	0.7290	0.7493
	$U = 1.3$	0.4450	0.4753	0.4441	0.4131	0.4569
	$U = 1.35$	0.1080	0.1174	0.1060	0.1104	0.1157
6m	$L = 1$	0.0248	0.0232	0.0224	0.0286	0.0003
	$L = 1.05$	0.0587	0.0640	0.0615	0.0585	0.0047
	$L = 1.1$	0.1218	0.1366	0.1318	0.1170	0.0360
	$L = 1.15$	0.2414	0.2591	0.2507	0.2317	0.1611
	$L = 1.2$	0.4812	0.5064	0.4879	0.4617	0.4634
	$U = 1.275$	0.8465	0.8602	0.8352	0.8149	0.8207
	$U = 1.3$	0.6308	0.6562	0.6170	0.5789	0.6000
	$U = 1.35$	0.2729	0.2918	0.2634	0.2538	0.2681
1y	$L = 1$	0.1087	0.1232	0.1197	0.1017	0.0104
	$L = 1.05$	0.1671	0.1872	0.1827	0.1600	0.0435
	$L = 1.1$	0.2577	0.2795	0.2718	0.2508	0.1331
	$L = 1.15$	0.4035	0.4280	0.4133	0.3934	0.3141
	$L = 1.2$	0.6296	0.6582	0.6389	0.6151	0.5961
	$U = 1.275$	0.9032	0.9051	0.8867	0.8719	0.8694
	$U = 1.3$	0.7684	0.7797	0.7466	0.7138	0.7092
	$U = 1.35$	0.5012	0.5115	0.4744	0.4399	0.4338
	$U = 1.4$	0.2866	0.2945	0.2693	0.2578	0.2377

We also present the pricing results for single-barrier reverse knock-in options as an example. The details of the knock-in options are shown in Table 3.7 and the computed prices from different models are given in Table 3.8. We can also conclude that the SLV model outperforms the other models in most cases.

Table 3.7: Parameter settings for EUR/USD single-barrier reverse knock-in options

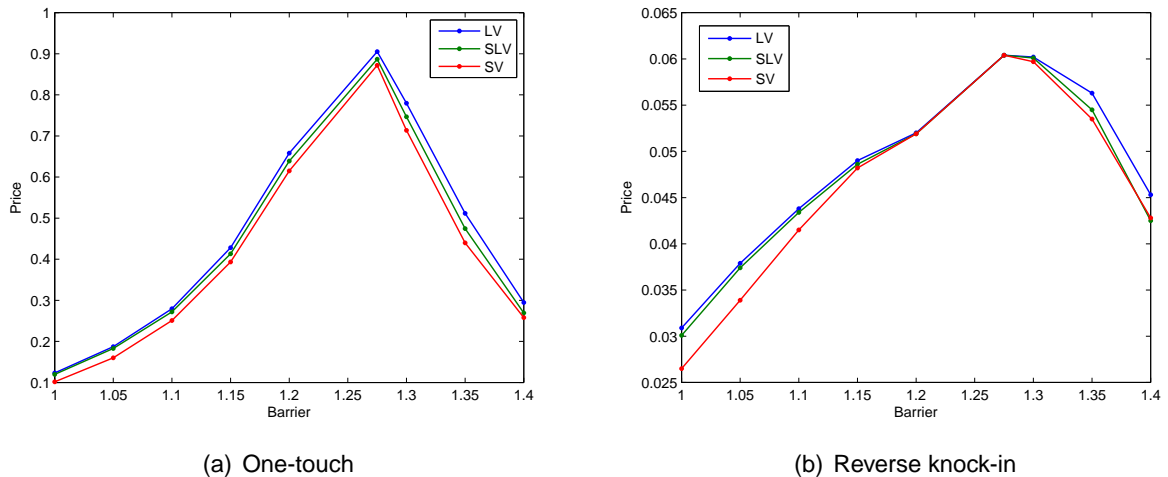
Maturity	1m, 3m, 6m and 1y
Spot	1.257 USD per EUR
Strike	1.255 USD per EUR
Lower trigger	$L = 1, 1.05, 1.1, 1.15$ and 1.2 , put options
Upper trigger	$U = 1.275, 1.3, 1.35$ and 1.4 , call options

We also compare the prices of one-touch and knock-in European options with different barrier from pure LV, SLV and pure SV (Heston) models in Figure 3.5. We can see that the prices from the SLV model is actually a non-linear combination of the prices from pure LV and pure SV models. Similar figures can be found in Section 8.5 of Clark [2011].

Table 3.8: Pricing results of EUR/USD single-barrier reverse knock-in options

Maturity	Trigger	Reference	LV	SLV	SV	TV
1m	$L = 1$	0.0000	0.0000	0.0000	0.0002	0.0000
	$L = 1.05$	0.0000	0.0000	0.0000	0.0002	0.0000
	$L = 1.1$	0.0000	0.0000	0.0000	0.0003	0.0000
	$L = 1.15$	0.0008	0.0004	0.0005	0.0012	0.0001
	$L = 1.2$	0.0063	0.0065	0.0063	0.0066	0.0043
	$U = 1.275$	0.0138	0.0139	0.0138	0.0136	0.0139
	$U = 1.3$	0.0086	0.0088	0.0083	0.0081	0.0090
	$U = 1.35$	0.0008	0.0006	0.0008	0.0010	0.0006
3m	$L = 1$	0.0003	0.0000	0.0000	0.0013	0.0000
	$L = 1.05$	0.0015	0.0009	0.0008	0.0027	0.0000
	$L = 1.1$	0.0050	0.0051	0.0049	0.0061	0.0005
	$L = 1.15$	0.0117	0.0131	0.0129	0.0122	0.0051
	$L = 1.2$	0.0195	0.0203	0.0202	0.0197	0.0169
	$U = 1.275$	0.0252	0.0255	0.0255	0.0254	0.0245
	$U = 1.3$	0.0226	0.0233	0.0225	0.0221	0.0227
	$U = 1.35$	0.0102	0.0111	0.0100	0.0112	0.0111
6m	$L = 1$	0.0066	0.0059	0.0058	0.0078	0.0001
	$L = 1.05$	0.0124	0.0130	0.0126	0.0125	0.0010
	$L = 1.1$	0.0194	0.0211	0.0206	0.0189	0.0055
	$L = 1.15$	0.0268	0.0277	0.0273	0.0263	0.0168
	$L = 1.2$	0.0325	0.0328	0.0327	0.0324	0.0273
	$U = 1.275$	0.0386	0.0386	0.0385	0.0385	0.0350
	$U = 1.3$	0.0376	0.0378	0.0373	0.0368	0.0342
	$U = 1.35$	0.0278	0.0286	0.0266	0.0269	0.0263
1y	$L = 1$	0.0284	0.0309	0.0301	0.0265	0.0026
	$L = 1.05$	0.0354	0.0379	0.0374	0.0339	0.0088
	$L = 1.1$	0.0424	0.0438	0.0434	0.0415	0.0203
	$L = 1.15$	0.0484	0.0490	0.0486	0.0482	0.0329
	$L = 1.2$	0.0518	0.0520	0.0519	0.0519	0.0394
	$U = 1.275$	0.0605	0.0604	0.0604	0.0604	0.0502
	$U = 1.3$	0.0602	0.0602	0.0601	0.0597	0.0499
	$U = 1.35$	0.0559	0.0563	0.0545	0.0535	0.0459
	$U = 1.4$	0.0451	0.0453	0.0425	0.0428	0.0357

Figure 3.5: Comparison of pricing results for EUR/USD 1y barrier options



4 Summary

In this paper, we presented our implementation of calibrating and pricing of the stochastic-local volatility model for FX options. The calibration of the SLV model splits in two parts: 1) calibrate

stochastic volatility parameters; and 2) calibrate leverage function. The first part can follow the conventional calibration approaches for term-structure Heston model. For the second calibration phase, a so-called mixing fraction parameter is introduced to control the weight of stochastic volatility and is calibrated to market implied volatilities and some exotic option prices from the market. During the second phase, the Fokker-Planck equation is solved repeatedly to produce the leverage function. After the stochastic parameters are calibrated and the leverage function is calculated, we can use the SLV model to price options.

References

- Carr, P. & Madan, D. B. [1999], 'Option valuation using the fast Fourier transform', *Journal of Computational Finance* **2**(4), 61–73.
- Clark, I. J. [2011], *Foreign Exchange Option Pricing: A Practitioners Guide*, John Wiley & Sons, West Sussex.
- Dupire, B. [1994], 'Pricing with a smile', *Risk* (January), 18–20.
- Elices, A. [2009], 'Affine concatenation', *Wilmott Journal* **1**(3), 155–162.
- Fang, F. & Oosterlee, C. W. [2008], 'A novel option pricing method for European options based on Fourier-cosine series expansions', *SIAM Journal on Scientific Computing* **31**(2), 826–848.
- Fang, F. & Oosterlee, C. W. [2011], 'A Fourier-based valuation method for Bermudan and barrier options under Heston's model', *SIAM Journal on Financial Mathematics* **2**(1), 439–463.
- Gatheral, J. [2006], *The Volatility Surface: A Practitioner's Guide*, John Wiley & Sons, Hoboken.
- Gyöngy, I. [1986], 'Mimicking the one-dimensional marginal distributions of processes having an Ito differential', *Probability Theory and Related Fields* **71**(4), 501–516.
- Hakala, J. & Wystup, U., eds [2007], *Foreign Exchange Risk: Models, Instruments and Strategies*, Risk Books, London.
- Heston, S. L. [1993], 'A closed-form solution for options with stochastic volatility with applications to bond and currency options', *Review of Financial Studies* **6**(2), 327–343.
- in't Hout, K. J. & Foulson, S. [2010], 'ADI finite difference schemes for option pricing in the Heston model with correlation', *International Journal of Numerical Analysis and Modeling* **7**(2), 303–320.
- Janek, A., Kluge, T., Weron, R. & Wystup, U. [2011], *Statistical Tools for Finance and Insurance*, 2nd edn, Springer, Berlin, chapter FX Smile in the Heston Model.
- Mikhailov, S. & Nögel, U. [2003], 'Heston's stochastic volatility model: Implementation, calibration and some extensions', *Wilmott magazine* (July), 74–79.
- Tachet, R. [2011], *Non-Parametric Model Calibration in Finance*, PhD thesis, Ecole Centrale Paris.
- Tataru, G. & Fisher, T. [2010], *Stochastic local volatility*. Bloomberg.
- Tavella, D. & Randall, C. [2000], *Pricing Financial Instruments: The Finite Difference Method*, John Wiley & Sons, New York.
- Wilmott, P. [2006], *Paul Wilmott on Quantitative Finance*, 2nd edn, John Wiley & Sons, West

Sussex.

CONTACT US

t 1300 363 400
+61 3 9545 2176
e enquiries@csiro.au
w www.csiro.au

YOUR CSIRO

Australia is founding its future on science and innovation. Its national science agency, CSIRO, is a powerhouse of ideas, technologies and skills for building prosperity, growth, health and sustainability. It serves governments, industries, business and communities across the nation.

FOR FURTHER INFORMATION

CSIRO Mathematics, Informatics and Statistics

Zili Zhu

t +61 3 9545 8003
e Zili.Zhu@csiro.au
w [Mathematics, Informatics and Statistics](#)